Direct thioether metathesis enabled by in situ formed Pd nanocluster catalysts

COMMUNICATION

Direct thioether metathesis enabled by in situ formed Pd nanocluster catalysts

Takehiro Matsuyama,[a] Takafumi Yatabe,*[ab] Tomohiro Yabe,[a] and Kazuya Yamaguchi*[a]

Thioether metathesis has been noted as a complementary thioether synthesis methodology with cross-coupling reactions, which can be applied to late-stage diversification. However, despite its utility, versatile direct C–S/C–S cross-metathesis of thioethers has not been previously reported. Herein, direct catalytic metathesis of various thioethers was enabled by Pd acetate and tricyclohexylphosphine precursors with no additives, affording unsymmetrical thioethers. Detailed characterization and control experiments confirmed that Pd(0) nanocluster homogeneous catalysts formed in situ are the actual active species enabling this versatile direct transformation. This work will pave the way for novel organic molecular transformations driven by metal nanocluster catalysts.

Introduction

Metathesis reactions, which involve the interchange of two functional groups between two reactants, are among the most powerful molecular transformations in synthetic organic chemistry.[1] Thioether metathesis in particular has attracted an increasing share of attention because late-stage diversification of already existing useful thioethers, which are widely found in polymers, natural products, bioactive compounds, and pharmaceuticals, will be enabled with the molecular frameworks intact.[2] In addition, thioether metathesis can be combined with well-developed C–S bond-formation methods such as cross-coupling reactions[2a,3] to widen the range of molecular transformations as the complementary functionalization approach (Scheme 1a),[1h] although thioether metathesis is an equilibrium reaction inherently affording the mixture of products and requiring driving force to push the equilibrium forward to achieve high yields. C–S bond metathesis of thioethers was pioneered by Morandi et al. in 2017, who demonstrated C–S/S–H metathesis between thiols and thioethers or thiols catalyzed by N-heterocyclic carbene (NHC)-ligated mononuclear Pd complexes.[4,5] However, this system requires an excessive amount of lithium bis(trimethylsilyl)amide (LiHMDS) to generate off-catalytic cycle byproducts that shift the equilibrium forward. Although metathesis via C–S bond scission has progressed since the first

efforts,[1h,6] few examples of thioether metathesis have been reported. In the reports by Morandi et al.[4,7] C–S/C–S cross-metathesis of thioethers was achieved via C–S/S–H metathesis between thioethers and thiol additives in the presence of a strong base (LiHMDS), which caused limited substrate scopes (Scheme 1b). To our knowledge, direct C–S/C–S cross-metathesis of diaryl thioethers has not been reported.

This study presents the first example of direct thioether metathesis in the presence of two catalyst precursors: palladium acetate (Pd(OAc)$_2$) and tricyclohexylphosphine (PCy$_3$).
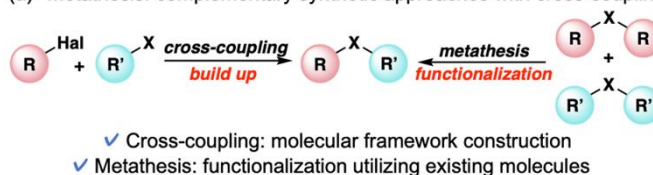
Scheme 1
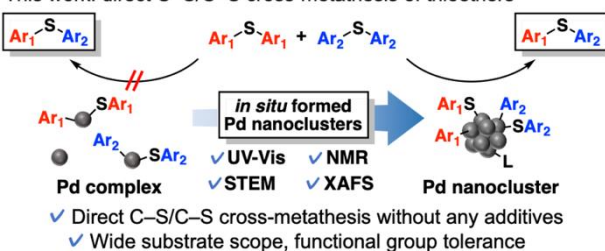
a. Department of Applied Chemistry, School of Engineering, The University of Tokyo, 7-3-1 Hongo, Bunkyo-ku, Tokyo 113-8656, Japan. E-mail: kyama@appchem.t.u-tokyo.ac.jp, yatabe@appchem.t.u-tokyo.ac.jp; Fax: +81-3-5841-7220.
b. Precursory Research for Embryonic Science and Technology (PRESTO), Japan Science and Technology Agency (JST), 4-1-8 Honcho, Kawaguchi, Saitama 332-0012, Japan.
† Footnotes relating to the title and/or authors should appear here.
Electronic Supplementary Information (ESI) available: [details of any supplementary information available should be included here]. See DOI: 10.1039/x0xx00000x

Scheme 1 Metathesis via C–S bond scission.

This system requires no thiols or strong base additives, which is advantageous for the selective transformations of complex molecules with base-sensitive or electrophilic functional groups. This catalytic system exhibits a wide substrate scope and functional group tolerance and achieves good to excellent product yields by utilizing Le Chatelier's principle. The actual active species in this reaction are not mononuclear Pd complexes but in situ formed Pd nanoclusters, which likely enable the efficient direct metathesis of thioethers (Scheme 1c). Despite outstanding properties of nanoclusters different from those of mononuclear complexes or bulk metal species,[8] most investigations of Pd nanocluster catalysts have focused on fundamental and well-developed molecular transformations including cross-coupling reactions.[9] Pd nanocluster catalysis in novel molecular transformations such as direct metathesis are underexplored so far. We also develop a previously unreported tandem reaction starting from two kinds of symmetrical thioesters, which affords unsymmetrical thioethers through decarbonylation/thioether metathesis.
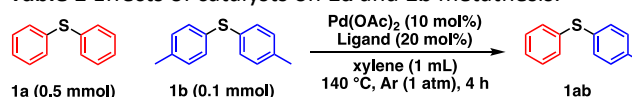
Results and Discussion

We initially investigated the effects of the catalysts on substrates of 0.5 mmol phenyl sulfide (**1a**) and 0.1 mmol *p*-tolyl sulfide (**1b**) under the conditions in Table 1. It should be noted the yield of **1ab** was calculated based on the two equivalents of **1b**, in other words, 0.2 mmol of **1ab** was produced from 0.1 mmol of **1b** if the metathesis proceeded quantitatively. After optimizing the conditions, namely, the temperature (Table S1), **1a/1b** ratio (Table S2), solvents (Table S3), and Pd catalyst amount/concentration (Table S4), the desired metathesis product phenyl *p*-tolyl sulfide (**1ab**) was obtained in 82% yield in the presence of Pd(OAc)₂ and PCy₃ (entry 1), whereas Ni and Rh complexes exhibited negligible catalytic performance (Table S5). After surveying different organic ligands with Pd(OAc)₂, we found that pyridine ligands or NHCs such as 4-dimethylaminopyridine (DMAP), 2,2'-bipyridyl (bpy), and 1,3-bis(2,6-diisopropylphenyl)imidazol-2-ylidene (IPr) are unsuitable (entries 2–4). PCy₃ achieved a higher **1ab** yield than the other phosphine ligands (entries 5–7). As **1ab** was hardly produced in the absence of Pd(OAc)₂, PCy₃, or both, Pd complexes with PCy₃ are involved in the active species (entries 8–10). The C–S/C–S cross-metathesis of diaryl thioethers by Morandi *et al*. requires thiols and LiHMDS for the intermediate C–S/S–H metathesis.[1h,4,7] In contrast, our catalytic system allows the direct C–S/C–S cross-metathesis without additives, suggesting direct cross-over between two oxidative adducts of thioethers. This direct metathesis reaction was confirmed to be reversible because the forward reaction (starting from **1a** (0.1 mmol) and **1b** (0.1 mmol)) and the reverse reaction (starting from **1ab** (0.2 mmol)) obtained almost the same ratios of **1a**, **1b**, and **1ab** (Table S6, entries 1 and 2). Moreover, an excessive amount of **1a** afforded a higher **1ab** yield than an equimolar mixture of **1a** and **1b** because excess **1a** shifted the equilibrium to the product side via Le Chatelier's principle (Table S6, entries 1 and 3). Therefore, a

large excess amount of one substrate is necessary for achieving high product yields.

When investigating the catalyst effects, we found a correlation between the color of the reaction solutions and catalytic activity. Rapid Pd black formation (entries 2, 3, 5, and 9; Scheme 2a) or a small color change (entries 4 and 6; Scheme 2b) signified a low catalytic activity. In contrast, a dramatic color change from yellow to dark red without precipitation (entries 1 and 7; Scheme 2c) was consistent with high **1ab** yield. Fig. 1a shows the time course data of C–S/C–S cross-metathesis under the optimized conditions. The reaction rate gradually accelerated after a certain induction period, which lengthened with increasing precursor ratio PCy₃/Pd(OAc)₂ (Fig. S1).

Motivated by these results, we sought the actual active species during the reaction. First, a hot-filtration test of the reaction solution confirmed the homogeneity of the observed catalysis (Fig. S2). Next, we measured the ultraviolet–visible absorption (UV–Vis) spectra of the reaction solution corresponding to the reaction profiles. The emerging broad absorption peaks around 400–550 nm in the UV–Vis spectra (Fig. 1b) are possibly assignable to ultra-small Pd(0) nanoclusters.[10,§] The appearance and growth of these peaks roughly

Table 1 Effects of catalysts on **1a** and **1b** metathesis.[a]

entry	metal source	ligand	conversion (%)		yield (%)
			1a	1b	1ab
1	Pd(OAc)₂	PCy₃	17	84	82
2	Pd(OAc)₂	DMAP	6	6	1
3	Pd(OAc)₂	bpy	8	11	2
4	Pd(OAc)₂	IPr	4	5	1
5	Pd(OAc)₂	PPh₃	4	13	5
6	Pd(OAc)₂	dcype	4	25	22
7	Pd(OAc)₂	dppe	8	56	53
8	–	PCy₃	<1	<1	<1
9	Pd(OAc)₂	–	2	6	3
10	–	–	<1	<1	<1

[a]Conditions: **1a** (0.5 mmol), **1b** (0.1 mmol), metal source (10 mol%), ligand (20 mol%), xylene (1 mL), Ar (1 atm), 140°C, 24 h. Conversions and yields were determined by GC. PPh₃ = triphenyl phosphine; dcype = 1,2-bis(dicyclohexylphosphino)ethane; dppe = 1,2-bis(diphenylphosphino)ethane.
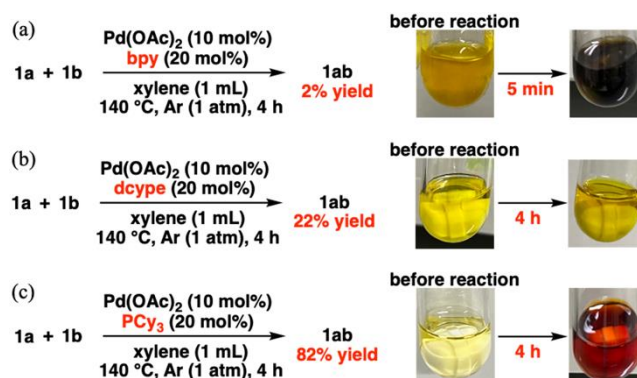
Scheme 2 Colors of the reaction solutions.

corresponded to the induction period and exponential acceleration, respectively, in the reaction profiles (Fig. 1a). According to the ^{31}P nuclear magnetic resonance (NMR)

spectra, Pd(OAc)$_2$(PCy$_3$)$_2$ (22 ppm) [11a] dominated in the initial state and the Pd(II) complex was almost completely consumed after 20 min, but peaks around 40 ppm assigned to Pd(PCy$_3$)$_2$ [11] were not
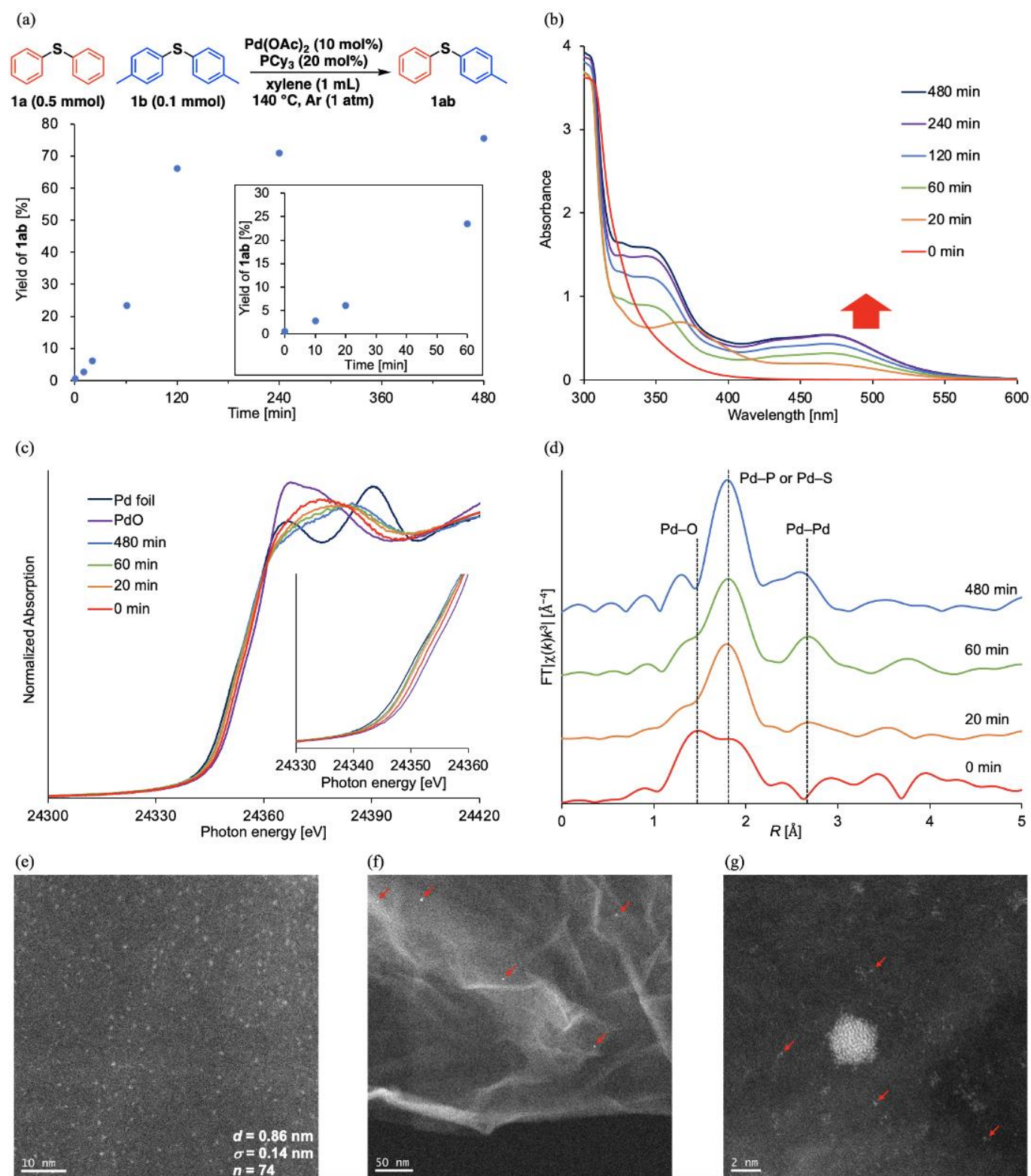

Fig. 1 Characterization of the reaction solutions: (a) reaction profiles of thioether metathesis between **1a** and **1b** under the indicated reaction conditions; (b) UV–Vis, (c) Pd K-edge XANES, and (d) k^3-weighted Fourier-transformed Pd K-edge EXAFS

spectra of the reaction solutions; HAADF–STEM images of (e) Pd nanoclusters, (f) Pd nanoparticles (pointed by red arrows), and (g) Pd mononuclear complexes (pointed by red arrows) in Pd/RGO.

observed. Instead, broad peaks around 46 ppm appeared in the ^{31}P NMR spectra at 1 h after starting the reaction (Fig. S3). The NMR spectra of ligands coordinating on nanocluster surfaces are typically broadened by changes in nanocluster size and coordination sites on the nanocluster surface.[12] Accordingly, the broad peaks around 46 ppm were attributed to coordination of PCy$_3$ on the Pd nanoclusters. Pd K-edge X-ray absorption near-edge structure (XANES) spectra of the reaction solutions were obtained at 0, 20, 60, and 480 min after starting the reaction. The Pd species in the reaction solutions were reduced after 20 min and the ratios of the reduced Pd species were almost maintained (Fig. 1c). Consistent with the ^{31}P NMR and XANES spectra, the k^3-weighted Fourier-transformed Pd K-edge extended X-ray absorption fine structure (EXAFS) spectra of the reaction solutions revealed scattering originating from disappearance of the Pd–O bond after 20 min (Fig. 1d). Additional scattering was derived from emergent Pd–Pd bonds in the reaction solution after 20 min of reaction. This scattering intensified at 60 and 480 min (Fig. 1d). As indicated in the wavelet transformed EXAFS oscillations, the intensity of the scatterings originating from Pd–Pd bonds gradually increased with reaction time (Fig. S4), consistent with the increase in the broad absorption peak assignable to Pd nanoclusters in the UV–Vis spectra. These observations suggest that catalytically

active Pd nanoclusters formed in the reaction solution. To directly observe the Pd nanoclusters, the Pd species in the reaction solutions were supported on reduced graphene oxide (Pd/RGO) via the equilibrium adsorption method at 1.5 h after starting the reaction.[§§] Ultra-small particles (mean diameter = 0.86 nm, standard deviation = 0.14 nm) were visible in the high-angle annular dark-field scanning transmission electron microscopy (HAADF–STEM) images of Pd/RGO (Figs. 1e and S5).[§§§] HAADF–STEM images after changing magnification also revealed small amounts of Pd nanoparticles (~2–5 nm, Fig. 1f)[§§§§, §§§§§] and mononuclear Pd species (Fig. 1g), but most of the Pd species apparently existed as Pd nanoclusters (Figs 1e–1g and S6), as also suggested by dynamic light scattering (DLS) measurements of the reaction solution.[§§§§§§] Therefore, Pd nanoclusters formed during the reaction are likely the actual active species of C–S/C–S cross-metathesis of thioethers and possibly enabled the efficient direct cross-over of multiple oxidative adducts on the Pd nanocluster surfaces.

Fig. 2a shows the substrate scope of the Pd-catalyzed C–S/C–S cross-metathesis of diaryl thioethers. The detailed amounts of thioethers after the reactions were summarized in Table S7. Unsymmetrical methyl-substituted phenyl sulfides in the *para*-, *meta*-, and *ortho*-positions of the aryl groups were synthesized (**1ab**–**1ad**). Thioethers with bulky substituents such
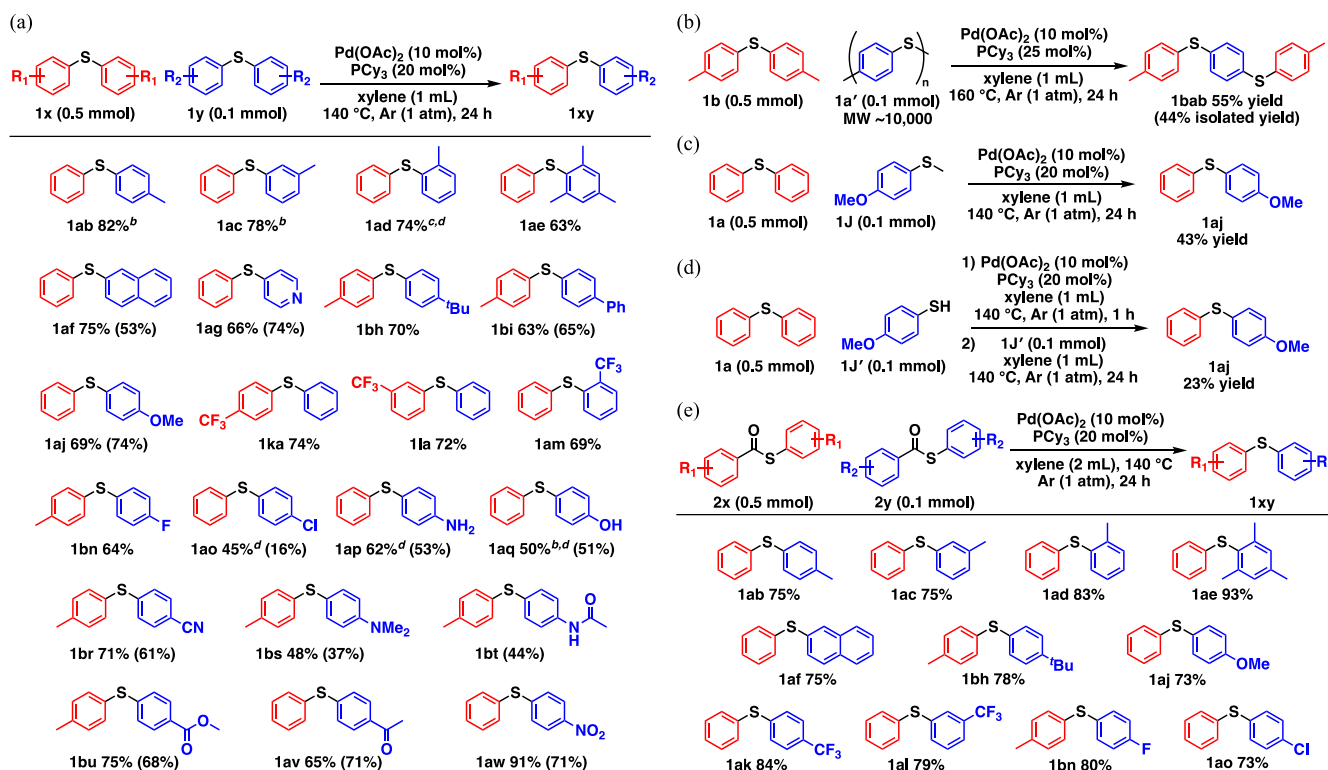

Fig. 2 Substrate scope: (a) Diaryl thioethers. ^{a}Conditions: **1x** (0.5 mmol), **1y** (0.1 mmol), Pd(OAc)$_2$ (10 mol%), PCy$_3$ (20 mol%), xylene (2 mL), 140°C. ^{b}Dioxane (2 mL). ^{c}Xylene (2 mL). ^{d}Pd(OAc)$_2$ (20 mol%), PCy$_3$ (40 mol%). (b) Polymer decomposition through C–S bond metathesis. The conditions are indicated in the scheme. (c) C–S/C–S cross-metathesis between **1a** and **1J**. The conditions are indicated in the scheme. (d) C–S/C–H metathesis between **1a** and **1J'**. The conditions were indicated in the

scheme. (e) Diaryl thioesters. Conditions: **2x** (0.5 mmol), **2y** (0.1 mmol), Pd(OAc)$_2$ (10 mol%), PCy$_3$ (20 mol%), xylene (2 mL), Ar (1 atm), 140°C, 24 h. Yields were determined by GC. Values in parentheses are isolated yields.

as 2,4,6-trimethyl phenyl groups afforded the corresponding metathesis product **1ae**. The catalytic system was also applicable to the 2-naphthyl group (**1af**) and the 4-pyridyl group (**1ag**). The metathesis of thioethers with *tert*-butyl (**1bh**), phenyl (**1bi**), methoxy (**1aj**), trifluoromethyl (**1ka**, **1la**, **1am**), fluoro (**1bn**), chloro (**1ao**), amino (**1ap**), phenolic hydroxy (**1aq**), cyano (**1br**), *N,N*-dimethylamino (**1bs**), acetamide (**1bt**), ester (**1bu**), acetyl (**1av**), and nitro (**1aw**) functional groups proceeded with their functional groups intact. Notably, the system accommodated base-sensitive functional groups such as phenolic hydroxyl (**1aq**), acetamide (**1bt**), and esters (**1bu**) because it directly achieves C–S/C–S cross-metathesis without LiHMDS. This reaction achieved gram-scale synthesis of **1aj** (1.03 g, 59% isolated yield, Scheme S1). In addition, when polyphenylenesulfide (**1a'**), a useful commercial thermoplastic polymer,[13] was subjected to the present metathesis with **1b** to recycle the polymer into other chemical building blocks, 1,4-bis[(4-methylphenyl)thio]benzene (**1bab**) was successfully obtained via polymer decomposition by consecutive thioether metathesis, which cannot be achieved by conventional thioether synthetic methods (Fig. 2b). C–S/C–S cross-metathesis between **1a** and 4-methoxy thioanisole (**1J**) also obtained an unsymmetrical diaryl thioether (**1aj**) (Fig. 2c, Scheme S2). Moreover, we investigated C–S/C–H metathesis starting from simultaneous placement of **1a** and 4-methoxybenzenethiol (**1J'**), but no reaction occurred, possibly because strong Pd–S bonding between the Pd complexes and **1J'** inhibited Pd nanocluster formation (Scheme S3). Once the Pd nanoclusters had formed, **1J'** addition afforded the C–S/C–H metathesis product **1aj** (Fig. 2d, Scheme S4).

The thioether moiety is obtained through decarbonylation of thioesters synthesized by carboxylic acid derivatives and thiols. In the presence of Pd-based catalysts, we demonstrated an unprecedented tandem reaction that affords unsymmetrical thioethers from two types of symmetrical thioesters. Fig. 2e summarizes the substrate scope of the tandem reaction. In all of the cases, thioesters were fully converted via decarbonylation, and the detailed amounts of thioethers after the reactions were summarized in Table S8. Symmetrical thioesters efficiently underwent decarbonylation/C–S bond metathesis to unsymmetrical thioethers, independently of the substituted position of the methyl group (**1ab**–**1ad**). The catalytic system was also applicable to the 2,4,6-trimethyl phenyl group (**1ae**) and the 2-naphthyl group (**1af**). Thioesters with *tert*-butyl (**1bh**), methoxy (**1aj**), trifluoromethyl (**1ak**, **1al**), fluoro (**1bn**), and chloro (**1ao**) groups also reacted well. Although decarbonylation of unsymmetrical thioesters to unsymmetrical thioethers in the presence of homogeneous Pd, Ni, or Rh catalysts is well-known, C–S bond metathesis proceeding from decarbonylated unsymmetrical thioethers has not been reported.[14]

Conclusions

In conclusion, we developed the first Pd-catalyzed direct C–S/C–S cross-metathesis of thioethers in the absence of thiol or basic additives. The catalytic system accommodates various thioethers, including those with base-sensitive functional groups. We also reported a novel tandem reaction (sequential decarbonylation/C–S bond metathesis) that synthesizes unsymmetrical thioethers. Through detailed characterization of the reaction solutions and a series of control experiments, we revealed that direct C–S/C–S cross-metathesis of thioethers was enabled by in situ formed Pd nanoclusters, which have multiple active surface sites. In general, the actual active species have barely been investigated in detail in previous developments of novel molecular transformations. In some cases, the actual active species, presumed as metal complexes in previous studies, might actually be in situ formed metal nanoclusters as observed here. This study demonstrated the unique catalysis of metal nanoclusters enabling unprecedented molecular transformations, which will afford a novel catalyst system design for the development of organic synthetic reactions.

Author Contributions

T.Yatabe and K.Y. conceived and supervised the project. T.M. performed most of the experiments. T.Yabe performed the XAFS measurements. All authors contributed to data analysis and discussed the results. T.M. and T.Yatabe wrote the manuscript with feedback from K.Y. and T.Yabe.

Conflicts of interest

There are no conflicts to declare.

Acknowledgements

was supported by the JSPS through the Research Fellowship for Young Scientists (Grant No. 23KJ0669).

Notes and references

§ The lack of any broad peaks in the UV–Vis spectra without **1a** and **1b** (Fig. S7) indicates that S-containing molecules are necessary for forming the possible Pd(0) nanoclusters.

§§ The UV-Vis spectrum of the reaction solution filtrate after being stirred with RGO showed slight decrease of overall peak intensities, indicating that a part of the Pd species were deposited on RGO and that the Pd nanoclusters still remained in the filtrate (Fig. S8). In addition, even in the filtrate, the metathesis reaction between **1a** and **1b** proceeded to reach the equilibrium, suggested that the addition of RGO did not much affect the Pd species structures in the reaction solution (Table S9).

§§§ The estimated diameter of Pd nanoclusters composed of 13 Pd atoms[15] approximates the present Pd nanocluster diameter, consistent with the similar broad peaks in the UV–Vis spectra of the present and previously reported[10] Pd_8 nanoclusters.

§§§§ Although a Pd nanocluster could not be mapped by STEM energy-dispersive X-ray spectroscopy (EDS) due to instability under electron irradiation, STEM–EDS mapping of a small nanoparticle (diameter ~2 nm) revealed Pd species ligated with S- and/or P-containing molecules (Fig. S9). The Pd nanoclusters probably have the same composition as the nanoparticles, as also implied by the Pd–P/Pd–S signals in the Pd K-edge EXAFS spectra of the reaction solutions (Fig. 1d) and the broad peaks assignable to P species coordinating with Pd nanoclusters in the ^{31}P NMR spectrum (Fig. S3).

§§§§§ Polyvinylpyrrolidone (PVP)-supported Pd nanoparticles and a heterogeneous hydroxyapatite-supported Pd nanoparticle catalyst (Pd/HAP) exhibited much lower catalytic performance than the in situ formed Pd nanoclusters (Table S10), indicating that a small amount of the observed Pd nanoparticles did not contribute to the high catalytic performance.

§§§§§§ Using DLS, we tried to measure the Pd nanoparticle size distribution in the reaction solution at 60 min of reaction under the conditions listed in Table 1. However, the DLS measurements failed, possibly because the main Pd species in the reaction solutions were very small like Pd nanoclusters.

1 (a) A. Fürstner, *Angew. Chem. Int. Ed.*, 2000, **39**, 3012–3043; (b) R. H. Grubbs, *Tetrahedron*, 2004, **60**, 7117–7140; (c) A. Fürstner, *J. Am. Chem. Soc.*, 2021, **143**, 15538–15555; (d) A. Fürstner, *Angew. Chem. Int. Ed.*, 2013, **52**, 2794–2819; (e) S. T. Diver and A. J. Giessert, *Chem. Rev.*, 2004, **104**, 1317–1382; (f) R. Waterman, *Organometallics*, 2013, **32**, 7249–7263; (g) Z. Lin, *Coord. Chem. Rev.*, 2007, **251**, 2280–2291; (h) B. N. Bhawal and B. Morandi, *Angew. Chem. Int. Ed.*, 2019, **58**, 10074–10103.

2 (a) C.-F. Lee, Y.-C. Liu and S. S. Badsara, *Chem. Asian J.*, 2014, **9**, 706–722; (b) K. L. Dunbar, D. H. Scharf, A. Litomska and C. Hertweck, *Chem. Rev.*, 2017, **117**, 5521–5577; (c) E. A. Ilardi, E. Vitaku and J. T. Njardarson, *J. Med. Chem.*, 2014, **57**, 2832–2842; (d) J. Lou, Q. Wang, P. Wu, H. Wang, Y.-G. Zhou and Z. Yu, *Chem. Soc. Rev.*, 2020, **49**, 4307–4359.

3 (a) P. Chauhan, S. Mahajan and D. Enders, *Chem. Rev.*, 2014, **114**, 8807–8864; (b) T. Kondo and T. Mitsudo, *Chem. Rev.*, 2000, **100**, 3205–3220; (c) S. V. Ley and A. W. Thomas, *Angew. Chem. Int. Ed.*, 2003, **42**, 5400–5449; (d) I. P. Beletskaya and V. P. Ananikov, *Chem. Rev.*, 2022, **122**, 16110–16293; (e) Z. Wu and D. A. Pratt, *Nat. Rev. Chem.*, 2023, **7**, 573–589; (f) V. J. Geiger, R. M. Oechsner, P. H. Gehrtz and I. Fleischer, *Synthesis*, 2022, **54**, 5139–5167; (g) R. M. Oechsner, I. H. Lindenmaier and I. Fleischer, *Org. Lett.*,

2023, **25**, 1655–1660; (h) G. Wang, L. Gao, Y. Feng and L. Lin, *Org. Lett.*, 2023, **25**, 4340–4344; (i) C. Liu, Y. Fang, S.-Y. Wang and S.-J. Ji, *ACS Catal.*, 2019, **9**, 8910–8915; (j) Sumit, D. Chandra, A. Thakur, A. K. Dhiman and U. Sharma, *J. Org. Chem.*, 2021, **86**, 13754–13761; (k) I. Chatterjee and G. Panda, *Org. Biomol. Chem.*, 2023, **21**, 3800–3810; (l) K. Ishitobi, K. Muto and J. Yamaguchi, *ACS Catal.*, 2019, **9**, 11685–11690.

4 Z. Lian, B. N. Bhawal, P. Yu and B. Morandi, *Science*, 2017, **356**, 1059–1063.

5 Before the pioneering work of Morandi *et al.*,[4] a very restricted example of C–S bond metathesis of thioethers was reported. See: M. Arisawa, Y. Tagami and M. Yamaguchi, *Tetrahedron Lett.*, 2008, **49**, 1593–1597.

6 (a) T. Delcaillau, A. Bismuto, Z. Lian and B. Morandi, *Angew. Chem. Int. Ed.*, 2020, **59**, 2110–2114; (b) T. Delcaillau, P. Boehm and B. Morandi, *J. Am. Chem. Soc.*, 2021, **143**, 3723–3728; (c) P. Boehm, P. Müller, P. Finkelstein, M. A. Rivero-Crespo, M.-O. Ebert, N. Trapp and B. Morandi, *J. Am. Chem. Soc.*, 2022, **144**, 13096–13108; (d) R. Isshiki, M. B. Kurosawa, K. Muto and J. Yamaguchi, *J. Am. Chem. Soc.*, 2021, **143**, 10333–10340; (e) K. Muto, R. Isshiki, M. B. Kurosawa and J. Yamaguchi, *Trends Chem.*, 2023, **5**, 102–103; (f) F. Bie, X. Liu, H. Cao, Y. Shi, T. Zhou, M. Szostak and C. Liu, *Org. Lett.*, 2021, **23**, 8098–8103; (g) K. Mitamura, T. Yatabe, K. Yamamoto, T. Yabe, K. Suzuki and K. Yamaguchi, *Chem. Commun.*, 2021, **57**, 3749–3752.

7 M. A. Rivero-Crespo, G. Toupalas and B. Morandi, *J. Am. Chem. Soc.*, 2021, **143**, 21331–21339.

8 (a) L. Liu and A. Corma, *Chem. Rev.*, 2018, **118**, 4981–5079; (b) L. Liu and A. Corma, *Trends Chem.*, 2020, **2**, 383–400; (c) Y. Du, H. Sheng, D. Astruc and M. Zhu, *Chem. Rev.*, 2020, **120**, 526–622; (d) U. Heiz and E. L. Bullock, *J. Mater. Chem.*, 2004, **14**, 564–577; (e) B. C. Gates, *Chem. Rev.*, 1995, **95**, 511–522; (f) J. Yang, F. Yang, C. Zhang, X. He and R. Jin, *ACS Materials Lett.*, 2022, **4**, 1279–1296; (g) Y. Cao, J.-L. Zhou, Y. Ma, Y. Zhou and J.-J. Zhu, *Dalton Trans.*, 2022, **51**, 8927–8937; (h) T. Kawawaki, A. Ebina, Y. Hosokawa, S. Ozaki, D. Suzuki, S. Hossain and Y. Negishi, *Small*, 2021, **17**, 2005328; (i) Y. Lu and W. Chen, *Chem. Soc. Rev.*, 2012, **41**, 3594–3623; (j) J. Cai, R. Javed, D. Ye, H. Zhao and J. Zhang, *J. Mater. Chem. A*, 2020, **8**, 22467–22487; (k) E. Fernández and M. Boronat, *J. Phys. Condens. Matter*, 2019, **31**, 013002.

9 (a) A. M. Trzeciak and A. W. Augustyniak, *Coord. Chem. Rev.*, 2019, **384**, 1–20; (b) A. Bej, K. Ghosh, A. Sarkar and D. W. Knight, *RSC Adv.*, 2016, **6**, 11446–11453; (c) M. T. Reetz and J. G. de Vries, *Chem. Commun.*, 2004, 1559–1563; (d) E. Fernández, M. A. Rivero-Crespo, I. Domínguez, P. Rubio-Marqués, J. Oliver-Meseguer, L. Liu, M. Cabrero-Antonino, R. Gavara, J. C. Hernández-Garrido, M. Boronat, A. Leyva-Pérez and A. Corma, *J. Am. Chem. Soc.*, 2019, **141**, 1928–1940; (e) A. Leyva-Pérez, J. Oliver-Meseguer, P. Rubio-Marqués and A. Corma, *Angew. Chem. Int. Ed.*, 2013, **52**, 11554–11559.

10 The absorption band of Pd nanoclusters composed of eight Pd atoms ligated by thiolates and phosphines (Pd_8) is centered at 487 nm in the following paper: S. Zhuang, D. Chen, Q. You, W. Fan, J. Yang and Z. Wu, *Angew. Chem. Int. Ed.*, 2022, **61**, e202208751.

11 (a) H. Hattori, Y. Ogiwara and N. Sakai, *Organometallics*, 2022, **41**, 1509–1518; (b) D. M. Norton, E. A. Mitchell, N. R. Botros, P. G. Jessop and M. C. Baird, *J. Org. Chem.*, 2009, **74**, 6674–6680; (c) A. L. Chan, J. Estrada, C. E. Kefalidis and V. Lavallo, *Organometallics*, 2016, **35**, 3257–3260; (d) H. Li, G. A. Grasa and T. J. Colacot, *Org. Lett.*, 2010, **12**, 3332–3335.

12 J. Zhang, Z. Li, K. Zheng and G. Li, *Phys. Sci. Rev.*, 2018, **3**, 20170083.

13 A. S. Rahate, K. R. Nemade and S. A. Waghuley, *Rev. Chem. Eng.*, 2013, **29**, 471–489.

14 (a) K. Osakada, T. Yamamoto and A. Yamamoto, *Tetrahedron Lett.*, 1987, **28**, 6321–6324; (b) H. Cao, X. Liu, F. Bie, Y. Shi, Y. Han, P. Yan, M. Szostak and C. Liu, *J. Org. Chem.*, 2021, **86**, 10829–10837; (c) T. Kato, H. Kuniyasu, T. Kajiura, Y. Minami, A. Ohtaka, M. Kinomoto, J. Terao, H. Kurosawa and N. Kambe, *Chem. Commun.*, 2006, 868–870; (d) N. Ichiishi, C. A. Malapit, Ł. Woźniak and M. S. Sanford, *Org. Lett.*, 2018, **20**, 44–47; (e) S.-F. Wang, C.-E. Li, Y.-C. Liu, D. M. Reddy, R. S. Basha, J. K. Park, S. Lee and C.-F. Lee, *Asian J. Org. Chem.*, 2020, **9**, 1826–1833; (f) H. Cao, X. Liu, F. Bie, Y. Shi, Y. Han, P. Yan, M. Szostak and C. Liu, *Org. Chem. Front.*, 2021, **8**, 1587–1592; (g) E. Wenkert and D. Chianelli, *J. Chem. Soc. Chem. Commun.*, 1991, 627–628; (h) C. Liu and M. Szostak, *Chem. Commun.*, 2018, **54**, 2130–2133; (i) K. Ishitobi, R. Isshiki, K. K. Asahara, C. Lim, K. Muto and J. Yamaguchi, *Chem. Lett.*, 2018, **47**, 756–759; (j) Z.-J. Zheng, C. Jiang, P.-C. Shao, W.-F. Liu, T.-T. Zhao, P.-F. Xu and H. Wei, *Chem. Commun.*, 2019, **55**, 1907–1910; (k) C. E. Brigham, C. A. Malapit, N. Lalloo and M. S. Sanford, *ACS Catal.*, 2020, **10**, 8315–8320; (l) J.-Y. Zhou, R. Tian and Y.-M. Zhu, *J. Org. Chem.*, 2021, **86**, 12148–12157; (m) T. Xu, X. Zhou, X. Xiao, Y. Yuan, L. Liu, T. Huang, C. Li, Z. Tang and T. Chen, *J. Org. Chem.*, 2022, **87**, 8672–8684.

15 M. Haruta, *J. Vac. Soc. Jpn.*, 2008, **51**, 721–726.